Journal of Molecular Modeling manuscript No.
(will be inserted by the editor)

Quantum treatment for internal rotations

Calculation of the two-dimensional non-separable partition function for two molecular systems

Luis Simón-Carballido · Antonio Fernández-Ramos

Received: date / Accepted: date

Abstract We present the application of an accurate quantum treatment, called two-dimensional non-separable (2D-NS), to the calculation of internal rotation partition functions of molecules with two rotors. This methodology involves full coupling in the kinetic and potential energies; the later is written as a Fourier series type potential. The resulting Hamiltonian is introduced in the Schrödinger equation and solved by the variational method. The method was applied to the 2-propenol and to the 3-fluoro-2-propenol molecular systems. The former molecule presents weak coupling between the torsion, whereas the later is an example of strong coupling. The comparison of 2D-NS with one-dimensional accurate models that involve separation of the two torsions, indicate that a separable model is inadequate to study systems in the strong coupling regime. The results indicate that for the case of strong coupling the multi-conformer harmonic approximation gives better results than a separable anharmonic model.

Keywords Internal rotations · Quantum partition function · Coupled torsions

1 Introduction

The rotation-vibration of molecules with hindered internal rotors has a long history [1, 2, 3]. General expressions using simple potentials were obtained by

Luis Simón-Carballido, Antonio Fernández-Ramos
Department of Physical Chemistry and Center for Research in Biological Chemistry and Molecular Materials (CIQUS), Universidade de Santiago de Compostela, 15782 Santiago de Compostela
Tel.: +34-881815705
Fax: +34-881815704
E-mail: qf.ramos@usc.es

Pitzer and Gwinn [4] and by Pitzer [5] for rigid frames with attached symmetrical and unsymmetrical rotors (or tops), respectively. Later on, Kilpatrick and Pitzer [6] considered even the most general case of rotating groups attached to other rotating groups, instead of to a rigid frame. Their method incorporates the coupling between different internal rotations to the kinetic energy, and if the potential is available, it allows to calculate accurate classical partition functions of the internal rotors. It is also possible to estimate the quantum partition function for internal rotation by multiplying the classical partition function by the coefficient resulting from the ratio between the quantum and classical harmonic-oscillator partition functions.

However, the calculation of an accurate quantum partition function, even for just two hindered rotors, is much more involved than that of its classical counterpart, because the former needs the calculation of a large number of energy levels, which are difficult to obtain. For the case of molecules with two internal rotors, which is the case we are studying here, important progress was made in the analysis of torsional spectra in molecules with certain symmetry (see for instance [7, 8, 9, 10, 11, 12]), in which the torsional potential is expressed as a Fourier series. In this work, we follow partially this strategy, in the sense that the potential is expanded in Fourier series, but the molecules and/or the rotating groups may not have any symmetry, and the analysis is not restricted to the first energy levels (as is the case in the analysis of spectra), but extended to the calculation of a large number of levels to obtain a converged quantum partition function for the two internal rotors.

In this context, the partition function that we outline in Sect. 2 (see Ref. [13] for a complete description) is called two-dimensional non-separable (2D-NS); it allows the calculation of accurate quantum partition functions of two tops including couplings in both the kinetic and potential energies. Sect. 3 describes an application of the 2D-NS method to two molecules, i.e., 2-propenol (**S1**), and 3-fluoro-2-propenol (**S2**) (Figure 1) for temperatures in the range between 100 and 2500 K. The former is a molecule with weak coupling between the two torsions, whereas the later involves moderate coupling. In Sect. 3, we also discuss the adequacy of using separable one-dimensional quantum partition functions for both molecules.

2 Methodology

2.1 Classical partition functions

For systems with two hindered rotors, ϕ_1 and ϕ_2, the classical partition function [14] is given by:

$$Q_{\mathrm{cl,tor}} = \frac{1}{\sigma_{\mathrm{tor}}} \frac{1}{2\pi\beta\hbar^2} \int_0^{2\pi} \int_0^{2\pi} d\phi_1 d\phi_2 |\mathbf{D}(\phi_1, \phi_2)|^{1/2} \mathrm{e}^{-\beta \mathrm{V}(\phi_1,\phi_2)} \qquad (1)$$

where $\beta = 1/k_B T$, k_B is the Boltzmann constant and T is the temperature; σ_{tor} is the symmetry number [15] for the two torsions; $V(\phi_1, \phi_2)$ is the potential

due to the two torsions; and $|\mathbf{D}(\phi_1,\phi_2)|^{1/2}$ is the square root of the determinant of the reduced $\mathbf{D}$ matrix, which includes the coupling in the kinetic energy [6]. The reduced $\mathbf{D}$ matrix is given by:

$$\mathbf{D}(\phi_1,\phi_2) = \begin{pmatrix} I_1(\phi_1,\phi_2) & -\Lambda_{1,2}(\phi_1,\phi_2) \\ -\Lambda_{1,2}(\phi_1,\phi_2) & I_2(\phi_1,\phi_2) \end{pmatrix} \tag{2}$$

being $I_1(\phi_1,\phi_2)$ and $I_2(\phi_1,\phi_2)$, the reduced moments of inertia calculated using the relations given by Pitzer [5], which are exact for molecules with one or more uncoupled internal rotors, and $\Lambda_{12}(\phi_1,\phi_2)$ is the coupling between the two reduced moments of inertia.

If the coupling in the kinetic and potential energies is neglected, the resulting classical partition function is separable, i.e.,

$$Q^{\mathrm{NC}}_{\mathrm{cl,tor}} = \frac{1}{\sigma_{\mathrm{tor}}} \frac{(I_1 I_2)^{1/2}}{2\pi\beta\hbar^2} \int_0^{2\pi} d\phi_1 e^{-\beta V_1^{1\mathrm{D}}(\phi_1)} \int_0^{2\pi} d\phi_2 e^{-\beta V_2^{1\mathrm{D}}(\phi_2)} \tag{3}$$

where I_1 and I_2 are the reduced moments of inertia of the two tops at the geometry of the absolute minimum; $V_1^{1\mathrm{D}}(\phi_1)$ and $V_2^{1\mathrm{D}}(\phi_2)$ are one-dimensional potentials.

2.2 Quantum partition functions

The 2D-NS partition function The Hamiltonian for two torsions, ϕ_1 and ϕ_2, that are coupled can be written as:

$$H_{\mathrm{tor}}\left(\tfrac{\partial}{\partial\phi_1}, \tfrac{\partial}{\partial\phi_2}; \phi_1, \phi_2\right) = T_{\mathrm{tor}}\left(\tfrac{\partial}{\partial\phi_1}, \tfrac{\partial}{\partial\phi_2}\right) + V_{\mathrm{tor}}(\phi_1,\phi_2) \tag{4}$$

where the kinetic energy T_{tor} is given by Eq. 8 of Ref. [13]. The potential energy $V_{\mathrm{tor}}(\phi_1,\phi_2)$ is split into three terms

$$V_{\mathrm{tor}}(\phi_1,\phi_2) = V_1(\phi_1) + V_2(\phi_2) + V^{2\mathrm{D}}(\phi_1,\phi_2), \tag{5}$$

and each of them is fitted to Fourier series:

$$V_1(\phi_1) = a_0 + \sum_{M=1}^{M_{\max}} a_M \cos(M\phi_1) + \sum_{M'=1}^{M'_{\max}} a'_{M'} \sin(M'\phi_1), \tag{6}$$

$$V_2(\phi_2) = b_0 + \sum_{N=1}^{N_{\max}} b_N \cos(N\phi_2) + \sum_{N'=1}^{N'_{\max}} b'_{N'} \sin(N'\phi_2), \tag{7}$$

and

$$
\begin{aligned}
V_{\mathrm{tor}}(\phi_1,\phi_2) = V_1(\phi_1) + V_2(\phi_2) + \\
\sum_{L_1=1}^{L_{1,\max}} \sum_{L_2=1}^{L_{2,\max}} c_{L_1L_2} \cos(L_1\phi_1)\cos(L_2\phi_2) + \\
\sum_{P_1=1}^{P_{1,\max}} \sum_{P_2=1}^{P_{2,\max}} d_{P_1P_2} \sin(P_1\phi_1)\sin(P_2\phi_2) + \\
\sum_{L'_1=1}^{L'_{1,\max}} \sum_{L'_2=1}^{L'_{2,\max}} c'_{L'_1L'_2} \cos(L'_1\phi_1)\sin(L'_2\phi_2) + \\
\sum_{P'_1=1}^{P'_{1,\max}} \sum_{P'_2=1}^{P'_{2,\max}} d'_{P'_1P'_2} \sin(P'_1\phi_1)\cos(P'_2\phi_2)
\end{aligned}
\tag{8}
$$

where a_0, b_0, $a_M(M = 1,\ldots,M_{\max})$, $a'_{M'}(M' = 1,\ldots,M'_{max})$, $b_N(N = 1,\ldots,N_{\max})$, and $b'_{N'}(N' = 1,\ldots,N'_{\max})$ are fitting parameters of the one-dimensional potential. Also $c_{L_1L_2}$, $L_1 = 1,\ldots,L_{1,\max}$, $L_2 = 1,\ldots,L_{2,\max}$, $d_{P_1P_2}, P_1 = 1,\ldots,P_{1,\max}, P_2 = 1,\ldots,P_{2,\max}$, $c'_{L'_1L'_2}$, $d'_{L'_1L'_2}$, $L'_1 = 1,\ldots,L'_{1,\max}$, $L'_2 = 1,\ldots,L'_{2,\max}$, and $d'_{P'_1P'_2}$, $P'_1 = 1,\ldots,P'_{1,\max}$, $P'_2 = 1,\ldots,P'_{2,\max}$ are fitting parameters, and $L_{1,\max}$, $L_{2,\max}$, $L'_{1,\max}$, $L'_{2,\max}$, $P_{1,\max}$, $P_{2,\max}$, $P'_{1,\max}$, and $P'_{2,\max}$ indicate the largest number of each series. It should be noticed that the potentials $V_1^{1\mathrm{D}}(\phi_1)$ and $V_2^{1\mathrm{D}}(\phi_2)$ are different from the potentials $V_1(\phi_1)$ and $V_2(\phi_2)$, because the former potentials correspond to one-dimensional potentials obtained by scanning one of the torsional angles while fixing the other, whereas the later are simply fitting potentials that, together with the potential of Eq. 8, minimize the root mean square of residuals with respect to the electronic structure calculations.

It is possible to solve the Schrödinger equation by the variational method using the product of two wavefunctions, and each of them is a linear combinations of the wavefunctions which are solution of the Schrödinger equation for the particle in a ring, i. e.,

$$\Phi(\phi_1,\phi_2) = \Phi_1(\phi_1)\Phi_2(\phi_2) \tag{9}$$

being

$$\Phi_1(\phi_1) = \frac{1}{\sqrt{2\pi}} \sum_{k=-k_{\max}}^{k_{\max}} c_{1,k} e^{ik\phi_1}, \tag{10}$$

and

$$\Phi_2(\phi_2) = \frac{1}{\sqrt{2\pi}} \sum_{n=-n_{\max}}^{n_{\max}} c_{2,n} e^{in\phi_2} \tag{11}$$

The trial wavefunction of Eq. 9 is used together with the Hamiltonian of Eq. 4 to obtain the eigenvalues. Thus, the 2D-NS quantum partition function

obtained from the direct sum of the eigenvalues is given by

$$Q_{\rm tor}^{\rm 2D-NS} = \frac{1}{\sigma_{\rm tor}} \sum_j e^{-\beta E_{{\rm tor},j}} \tag{12}$$

where

$$\sigma_{\rm tor} = \sigma_1 \sigma_2 \tag{13}$$

being σ_1 and σ_2 the symmetry numbers associated to the internal rotation about ϕ_1 and ϕ_2, respectively, and $E_{{\rm tor},j}$ the j-th eigenvalue.

The separable torsional partition function In the case of two independent torsions, the Hamiltonian of Eq. 4 is separable and reduces to

$$H_{\rm tor}^{\rm STES} = \frac{-\hbar^2}{2} \sum_{\tau=1}^{2} \left\{ \frac{1}{I_\tau} \frac{d^2}{d\phi_\tau^2} \right\} + V_\tau^{\rm 1D}(\phi_\tau) \tag{14}$$

where STES stands for separable torsional eigenvalue summation [16]; I_τ, $\tau = 1, 2$ are the reduced moments of inertia of the two torsions, and $V_\tau^{\rm 1D}(\phi_\tau)$ are the one-dimensional potentials generated by rotation about each of the two tops. The two separable Schrödinger equations are obtained from the Hamiltonians of Eq. 14 and can be solved by the variational method using as trial functions Eqs. 10 and 11. The partition function of torsion τ is given by

$$q_\tau^{\rm TES} = \frac{1}{\sigma_\tau} \sum_j e^{-\beta \varepsilon_{\tau,j}}, \tag{15}$$

being σ_τ the symmetry number for the internal rotation and $\varepsilon_{\tau,j}$ the j-th eigenvalue. The resulting STES partition function of the two internal rotations is:

$$Q_{\rm tor}^{\rm STES} = \sum_{\tau=1}^{2} q_\tau^{\rm TES} \tag{16}$$

It should be noticed that Eq. 12 reduces to Eq. 1 and that Eq. 16 reduces to Eq. 3 in the limit of high temperatures.

2.3 Computational details

All the electronic structure calculations were performed at the MPWB1K method [17] with the augmented polarized double-ζ basis set, 6-31+G(d,p) [18]. The geometries of all the minima (with the exception of enantiomers) for the two molecules are depicted in Fig. 1 and listed in the Supplementary Material. All normal-mode frequencies were scaled by 0.964 [19]. The two-dimensional torsional potential energy surfaces for the two systems were generated by optimizing all the degrees of freedom but the two torsions, using a stepsize of 10°. The potential was fitted to Fourier series using the Gnulot [20] program with

a root mean square of residuals smaller than 8 cm^{-1}. The parameters of the fit for the potential of Eqs 5 and 14 are listed in the Supplementary Material.

The classical partition functions were evaluated by numerical integration using the trapezoidal rule with a stepsize of 1°. This fine grid was obtained by fitting the electronic structure calculations to a spline under tension [21].The calculation of the eigenvectors was carried out with the help of the JADAMILU software library [22]. The calculation of the $Q_{\rm tor}^{\rm 2D-NS}$ and $Q_{\rm tor}^{\rm STES}$ partition functions was carried out by the HR2D program [23].

3 Applications

The equilibrium conformations are depicted in Fig. 1 and the energetics of those conformations together with the value of the two torsional angles is given in Table 1. The torsional angles ϕ_1 and ϕ_2 are measured about atoms labeled in Fig. 1 as 1, 2, 3, 4, and 1, 2, 5, 6, respectively. It should be noticed that **S1** only has two distinguishable minima with C_s symmetry, which correspond to two planar dispositions of the -OH group. The rotation of the methyl group generates 3 indistinguishable minima, and therefore the internal rotation about this group has a symmetry number $\sigma_2 = 3$. For system **S2** the symmetry of the internal rotation about the partially substituted methyl group disappears and all the conformers derived from the rotation of this group correspond to distinguishable conformations. Structure **S2-M1** belongs to the C_s point group symmetry, but the other three structures do not have any symmetry and therefore each of them has one enantiomer. As shown in Fig. 2 the presence of the fluorine atom introduces coupling between the two torsions ([ϕ_1, ϕ_2]) because the most stable structure is located at [0, 0], as for system **S1**, but structures with ϕ_2 close to zero degrees are destabilized with respect to the same structures in **S1**, whereas structure **S2-M2** located at [199, 142] is much more stable than [180, 120] in **S1**. The reason is that the fluorine atom forms strong hydrogen bonds in structures **S2-M1** and **S2-M2** and, therefore, the one-dimensional potential for ϕ_1, which starts at 360 degrees (Fig. 2) and moves to 199° and to 161° degrees, finishes in zero degrees. This is a clear indication that the coupling between the internal rotations in **S2** is strong, because on the contrary of what occurs for **S1**, the variation of ϕ_1 affects ϕ_2 and vice-versa.

Table 2 lists the normal-mode frequencies, $\omega_{i,1}$, and $\omega_{i,2}$, obtained at the MPWB1K/6-31+G(d,p) level and the torsional frequencies obtained from the second derivatives of the torsional potential of Eq. 5. Specifically, these frequencies, $\overline{\omega}_{i,1}$, and $\overline{\omega}_{i,2}$, are calculated from the the eigenvalues of the secular determinant involving the **D** matrix and from the torsional force constants matrix, [5] i.e.,

$$|\mathbf{K} - \overline{\omega}_\tau \mathbf{D}| = 0 \tag{17}$$

being

$$\mathbf{K} = \begin{pmatrix} \frac{\partial^2 V}{\partial \phi_1^2} & \frac{\partial^2 V}{\partial \phi_1 \partial \phi_2} \\ \frac{\partial^2 V}{\partial \phi_1 \partial \phi_2} & \frac{\partial^2 V}{\partial \phi_2^2} \end{pmatrix} \tag{18}$$

In general, the normal mode frequencies and the the torsional frequencies are quite similar for the two systems, which indicates that the normal modes associated to the torsions are almost pure motions and with little participation by other vibrational degrees of freedom. It is also interesting to compare the 2D-NS partition function with the harmonic oscillator (HO) partition function. However, the potential energy surfaces of Fig. 2 have more than one minima, so it is more accurate to define multi-conformational harmonic oscillator (MC-HO) partition functions for the both types of frequencies. For the case of torsional frequencies the MC-HO partition function is given by

$$\overline{Q}_{\rm tor}^{\rm MC-HO} = \sum_{i=1}^{n_{\rm C}} e^{-\beta U_i} \prod_{\tau=1}^{2} \overline{q}_{i,\tau}^{\rm HO} \tag{19}$$

where the sum runs over the number of distinguishable conformers, $n_{\rm C}$; U_i is the difference in energy between conformers listed in Table 2; each of the two individual HO partition functions $\overline{q}_{i,\tau}^{\rm HO}$ of the i-th conformer is given by

$$\overline{q}_{i,\tau}^{\rm HO} = \frac{e^{-\beta\hbar\overline{\omega}_{i,\tau}/2}}{1-e^{-\beta\hbar\overline{\omega}_{i,\tau}}}, \tag{20}$$

In a equivalent manner, the MC-HO partition function is

$$Q_{\rm tor}^{\rm MC-HO} = \sum_{i=1}^{n_{\rm C}} e^{-\beta U_i} \prod_{\tau=1}^{2} q_{i,\tau}^{\rm HO} \tag{21}$$

being $q_{i,\tau}^{\rm HO}$ the individual partition function of torsion τ of the i-th conformer, which is given by Eq. 21 but using normal-mode frequencies. Tables 3 and 4 show the ratio between the 2D-NS partition function and the two MC-HO partition functions of Eqs. 19 and 21. The two ratios are quite similar and follow the same tendency, although the $\overline{Q}_{\rm tor}^{\rm MC-HO}$ partition function is closer in value to 2D-NS. Both ratios are larger than unity except at very high temperatures that are smaller than unity; this is because at high temperatures the density of states is larger for the HO because the space available to the molecular system in the torsional potential is larger than that of parabolic potentials. For system **S1** the torsional potential (Fig. 2) has lower barriers than system **S2** and thus the temperature at which the ratio becomes smaller than unity is lower for **S1** than for **S2**. The major deviations from unity occur at temperatures between 300 and 1000 K, but in general the MC-HO approximation gives reasonable results.

The zero-point energies obtained by STES and 2D-NS are also quite similar, which may induce us to think that STES is a good approximation for both systems. However, these results are deceiving because the ground state is just the first of a large number of states that contribute to the partition function. In fact, the STES approximation, which considers that the two torsions can be treated as independent rotors, works well for **S1**, because the coupling is weak, but it is very inaccurate for **S2**, which a system with strong coupling. Thus, at $T = 300$ K the STES value is more than double the one obtained

by the 2D-NS method. The one-dimensional potentials used to calculate the STES partition function for **S2** are depicted in Fig. 2; they are calculated by following one of the torsional angles while fixing the other. Unfortunately, these one-dimensional potentials cannot reproduce all the features of the two-dimensional potential, and because they were obtained from the minimization of the other torsional angle (following the energetically most favorable path), the STES partition function greatly overestimates the accurate value. In fact, the results indicate, that for the case of strong coupling, the MC-HO partition function, in whichever of the two versions given above, gives better results than the STES partition function.

The coupling in the kinetic energy has a weak effect in the partition functions. It can be estimated by substituting the **D** matrix in Eq. 1 by the reduced moments of inertia of the absolute minimum. We have found out that this effect is negligible for **S1** and that oscillates between about 3% at $T = 100$ K and 6% at $T = 2500$ K for **S2**. Finally, it should be mentioned that the accurate classical partition function reduces to the quantum partition function quite above room temperature and therefore it is important to take into account quantum effects till at least $T = 500$ K.

Acknowledgements The authors thank the Centro de Supercomputación de Galicia (CESGA) for computational facilities.

References

1. Dennison DM (1926) The rotation of molecules. Phys Rev 28:318–333.
2. Nielsen HH (1932) The torsion oscillator-rotator in the quantum mechanics. Phys Rev 40:445–456.
3. Crawford Jr. BR (1939) The partition functions and energy levels of molecules with internal torsional motions. J Chem Phys 8:273–281.
4. Pitzer KS, Gwinn WD (1942) Energy levels and thermodynamic functions for molecules with internal rotations. I. Rigid frame with attached tops. J Chem Phys 10:428–440.
5. Pitzer KS (1946) Energy levels and thermodynamic functions for molecules with internal rotations. II. Unsymmetrical tops attached to a rigid frame. J Chem Phys 14:239–243.
6. Kilpatrick JE, Pitzer KS (1949) Energy levels and thermodynamics functions for molecules with internal rotation. III. Compound rotation. J Chem Phys 17:1064–1075.
7. Groner P, Durig JR (1977) Anaysis of torsional spectra of molecules with two internal C_3v rotors. II. Far infrared and low frequency Raman spectra of dimethylether isotopes. J Chem Phys 66:1856–1874.
8. Durig JR, Griffin MG, Groner P (1977) Analysis of torsional spectra of molecules with two internal C_3v rotors. III. Far infrared and gas phase Raman spectra of dimethylamine-d_0,-d_3 and -d_6. J Phys Chem 81:554–560.

9. Durig JR, Groner P, Griffin MG (1977) Analysis of torsional spectra of molecules with two C_3v internal rotors. IV. The torsional potential function for propane-d_0 and -d_3. J Chem Phys 66:3061–3065.
10. Smeyers YG, Bellido MN (1981) Internal dynamics of nonrigid molecules. I. Application to acetone. Int J Quantum Chem 19:553–565.
11. Smeyers YG, Bellido MN (1983) Potential energy surface determinations for nonrigid molecules: application to acetone. Int J Quantum Chem 23: 507–516.
12. Maruani J, Smeyers YG, Hernández-Laguna A (1982) The influence of symmetry on the conformational dependences of scalar and vectorial properties for double rotor molecules. J Chem Phys 76:3123–3130.
13. Fernández-Ramos A (2013) Accurate treatment of two-dimensional nonseparable hindered internal rotors. J Chem Phys 138:134112–10.
14. Edinoff ML, Aston JG (1935) The rotational entropy of nonrigid polyatomic molecules. J Chem Phys 3:379–383.
15. Fernández-Ramos A, Ellingson BA, Meana-Pañeda R, Marques JMC, Truhlar DG (2007) Symmetry numbers and chemical reaction rates. Theor Chem Acc 118:813–826.
16. Ellingson BA, Lynch VA, Mielke SL, Truhlar DG (2006) Statistical thermodynamics of bond torsional modes: Tests of separable, almost-separable, and improved Pitzer–Gwinn approximations. J Chem Phys 125:84305-17.
17. Zhao Y, Lynch BJ, Truhlar DG (2004) Hybrid Meta Density Functional Theory methods for Thermochemistry, Thermochemical Kinetics, and noncovalent interactions: The MPW1B95 and MPWB1K models and comparative assessments for hydrogen bonding and van der Waals interactions. J Phys Chem A 108:6908–6918.
18. Hehre WJ, Ditchfield R, Pople JA (1972) Self-consistent molecular orbital methods. XII. Further extensions of Gaussian type basis sets for use in molecular orbital studies of organic molecules. J Chem Phys 56(5):2257–2260.
19. Alecu IM, Zheng J, Zhao Y, Truhlar DG (2010) Computational thermochemistry: Scale factor databases and scale factors for vibrational frequencies obtained from electronic model chemistries. J Chem Theory Comput 6:2872–2887.
20. Gnuplot version 4.2; http://www.gnuplot.info; nov. 2012.
21. Renka RJ (1993) Algorithm 716. TSPACK: Tension spline curve-fitting package. ACM Trans Math Software 19(1):81–94.
22. Bollhöfer M, Notay Y (2007) Jadamilu: A software code for computing selected eigenvalues of large sparse symmetric matrices. Comput Phys Commun 177:951–964.
23. Fernández-Ramos A (2013) HR2D version 1.0, Universidade de Santiago de Compostela, Santiago de Compostela.

Table 1 Some parameters of interest for the two internal rotations of the two systems, i.e., total number of wells, the symmetry numbers for internal rotation, and the energy difference between conformers U_i (in cm^{-1}). It also indicates if a given structure has an enantiomer and the two torsional angles ϕ_1, ϕ_2. For the other enantiomer $\phi_1 \to 360 - \phi_1$ and $\phi_2 \to 360 - \phi_2$

System	Wells	σ_1, σ_2	Conformer	Enantiomer?	$[\phi_1, \phi_2]$	U_i
S1	6	1, 3	**S1-M1**	No	0, 0	0
		1, 3	**S1-M2**	No	180, 0	781
S2	7	1, 1	**S2-M1**	No	0, 0	0
			S2-M2	Yes	199, 142	50
			S2-M3	Yes	6, 242	439
			S2-M4	Yes	156, 354	1273

Table 2 List of the normal-mode frequencies $\omega_{i,1}$ and $\omega_{i,2}$ and torsional frequencies $\overline{\omega}_{i,1}$ and $\overline{\omega}_{i,2}$ of all conformations. The torsional frequencies were calculated by Eq. 17. The zero-point energies (ZPE) calculated by the STES and 2D-NS methods are also indicated. All the frequencies and ZPEs are given in cm^{-1}. The reduced moments of inertia are given in amu·Å^2

System	ZPE^{STES}	ZPE^{2D-NS}	Conformer	$\omega_{i,1}, \omega_{i,2}$	$\overline{\omega}_{i,1}, \overline{\omega}_{i,2}$	I_1, I_2
S1	298	293	**S1-M1**	424, 181	419, 180	0.743, 2.937
			S1-M2	214, 169	233, 178	0.737, 2.930
S2	226	233	**S2-M1**	373, 108	368, 101	0.761, 10.87
			S2-M2	425, 118	432, 119	0.777, 13.13
			S2-M3	399, 91	390, 81	0.753, 13.18
			S2-M4	217, 112	229, 103	0.740, 10.82

Table 3 Quantum 2D-NS partition function at different temperatures and different rations between Q^{2D-NS} and the partition functions of Eqs. 1, 3, 16, 21, and 19 for system **S1**

T(K)	Q^{2D-NS}	$\frac{Q^{2D-NS}}{Q_{cl,tor}}$	$\frac{Q^{2D-NS}}{Q^{NC}_{cl,tor}}$	$\frac{Q^{2D-NS}}{Q^{STES}_{tor}}$	$\frac{Q^{2D-NS}}{Q^{MC-HO}_{tor}}$	$\frac{Q^{2D-NS}}{\overline{Q}^{MC-HO}_{tor}}$
100	0.0163	0.25	0.27	1.09	1.17	1.12
150	0.0776	0.51	0.54	1.06	1.14	1.11
200	0.188	0.68	0.71	1.04	1.14	1.12
250	0.348	0.78	0.81	1.03	1.14	1.12
300	0.563	0.85	0.86	1.02	1.15	1.13
400	1.18	0.92	0.92	1.00	1.14	1.15
500	2.07	0.95	0.94	0.99	1.14	1.16
700	4.79	0.98	0.96	0.98	1.12	1.15
1000	11.3	1.00	0.97	0.98	1.08	1.13
1500	27.3	1.00	0.97	0.97	0.97	1.02
2000	47.8	1.00	0.97	0.97	0.86	0.92
2500	71.4	1.00	0.98	0.98	0.77	0.83

Table 4 Same as Table 3 but for system **S2**

T(K)	$Q^{\mathrm{2D-NS}}$	$\frac{Q^{\mathrm{2D-NS}}}{Q_{\mathrm{cl,tor}}}$	$\frac{Q^{\mathrm{2D-NS}}}{Q_{\mathrm{cl,tor}}^{\mathrm{NC}}}$	$\frac{Q^{\mathrm{2D-NS}}}{Q_{\mathrm{tor}}^{\mathrm{STES}}}$	$\frac{Q^{\mathrm{2D-NS}}}{Q_{\mathrm{tor}}^{\mathrm{MC-HO}}}$	$\frac{Q^{\mathrm{2D-NS}}}{\overline{Q}_{\mathrm{tor}}^{\mathrm{MC-HO}}}$
100	0.0767	0.33	0.19	0.43	1.20	1.13
150	0.352	0.58	0.29	0.43	1.17	1.12
200	0.871	0.73	0.34	0.43	1.17	1.13
250	1.67	0.82	0.38	0.44	1.18	1.13
300	2.77	0.87	0.41	0.45	1.19	1.15
400	6.04	0.93	0.45	0.47	1.22	1.17
500	10.9	0.96	0.48	0.50	1.24	1.19
700	26.0	0.98	0.55	0.55	1.27	1.21
1000	63.0	1.00	0.63	0.63	1.27	1.20
1500	155	1.00	0.72	0.72	1.17	1.10
2000	277	1.00	0.78	0.78	1.06	1.00
2500	418	1.00	0.83	0.83	0.95	0.90

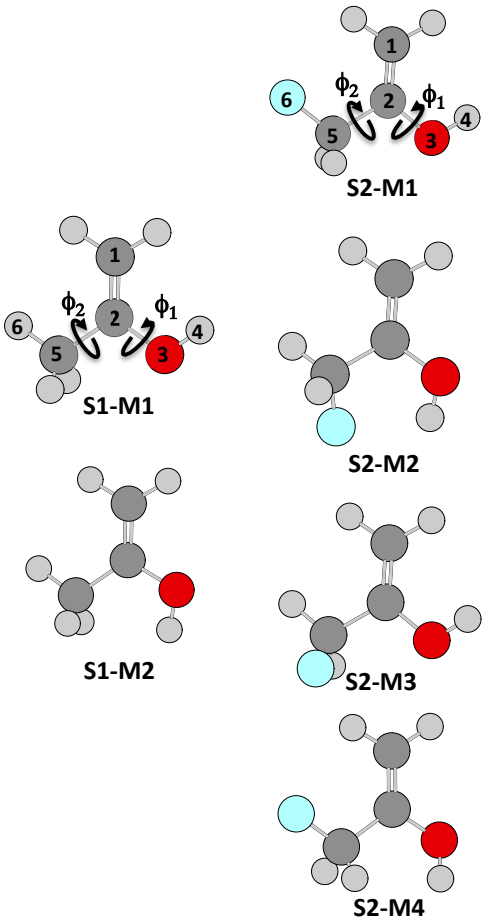

Fig. 1 Schematic depiction of the equilibrium conformers of **S1** and **S2**. Dark gray, light gray, red and cyan represent carbon, hydrogen, oxygen and fluorine atoms, respectively. Torsional angles: ϕ_1 about atoms with 1, 2, 3, 4 labels; ϕ_2 about atoms with 1, 2, 5, 6 labels.

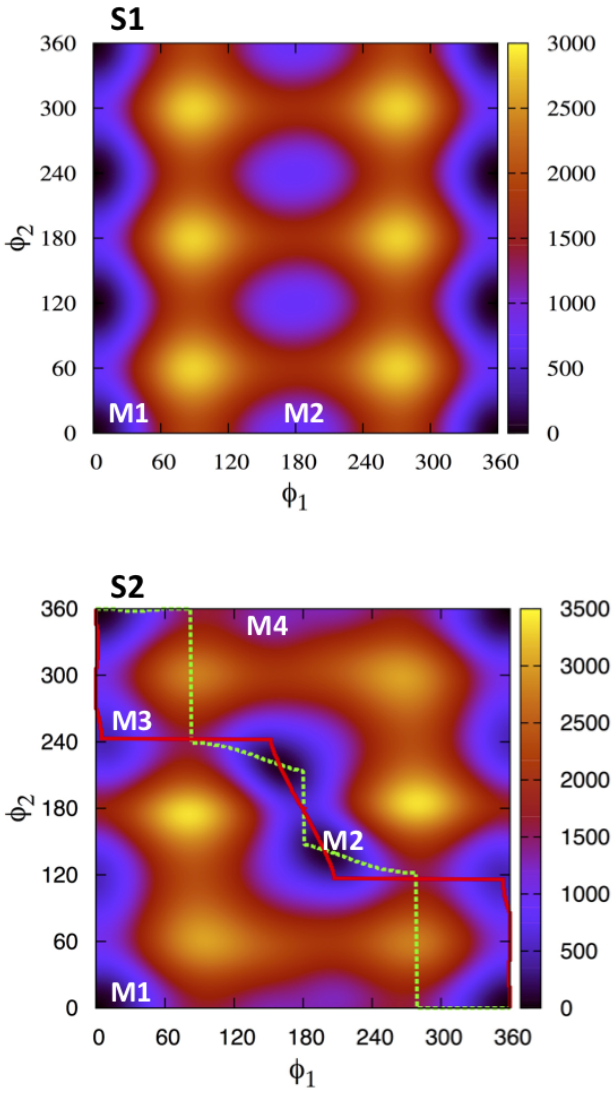

Fig. 2 Contour plot of the potential energy for the rotation about torsional angles ϕ_1 and ϕ_2. The location of the minima is also indicated. For structures with only one enantiomer or for structures that are indistinguishable only one conformation is indicated. The dashed-green and solid-red lines in **S2** indicate the one-dimensional potentials about ϕ_1 and ϕ_2, respectively.